no. 3, serum estradiol was transiently detected above 20 pg/ml, but she did not resume menstruating.

Assessment of basal body temperature and monitoring of follicle growth by sonohysterography would be useful to assess ovarian function of patients undergoing ovarian shielding in TBI.

Actual measurement for phantom

The mean and median actual doses measured by means of the glass dosimeters, which were inserted in the position of the ovaries in the humanoid phantom were between 1.041 and 1.042 Gy, respectively with a prescribed dose of 4 Gy. The range was 9.98–1.096 Gy. The results meant that the average total dose of the ovary was reduced from 12 to 3.123 Gy (74% less).

Discussion

The dose-limiting toxicity of TBI is interstitial pneumonia. Although the incidence of interstitial pneumonia has been significantly reduced by the use of fractionated irradiation compared to single dose irradiation,[13] 15% of patients still develop interstitial pneumonia after fractionated TBI. Therefore, lung shielding has been investigated to decrease lung toxicity of TBI. In a small nonrandomized study, the incidence of interstitial pneumonia was lower in patients who underwent TBI with lung shielding than in those who did not have shielding.[14] TBI may also affect renal function after transplantation. Therefore, Lawton *et al.*[15] attempted to protect renal function by renal shielding decreasing the total dose to the kidneys from 14 to 12 Gy, and the incidence of late renal dysfunction decreased from 26 to 6%.

The ovary is an organ sensitive to irradiation and the number of antral follicles per ovary has been shown to be reduced by ovarian irradiation in long-term survivors of childhood cancer.[16] Also, Shuck *et al.*[17] reported that all patients who received irradiation to the ovaries at greater than 15 Gy developed hormone failure. The radiation doses that cause 5 and 50% complications to the ovaries are about 3 and 10 Gy, respectively.[18] In this study, the irradiation dose to the ovaries was decreased by 75% by ovarian shielding and the total dose to the ovaries was estimated at about 3 Gy. Considering that recovery of ovarian function is frequently observed after a conditioning regimen of cyclophosphamide at 200 mg/kg only, the combination of cyclophosphamide at 120 mg/kg and TBI at 12 Gy with ovarian shielding should be reasonably protective to the ovaries.

Although patients who have received a conditioning regimen of cyclophosphamide and TBI may have spontaneous recovery of ovarian function long after transplantation, the incidence is less than 15% and it takes a median of 5 years for recovery of ovarian function after transplantation.[19] In this study, regular menstruation recovered in two of the three patients within 2 years after transplantation, showing the protective effect of ovarian shielding. However, spontaneous recovery of ovarian function is rarely seen after a combination of busulfan and cyclophosphamide, another major conditioning regimen for leukemia.[19 22] The risk of persistent alopecia is also more frequent after a busulfan-containing regimen.[23] Therefore, the combination of busulfan and cyclophosphamide should be avoided in young female patients, unless the patient has a condition that precludes the use of TBI, such as previous high-dose irradiation to a major organ.

It remains to be seen whether the recovery of ovarian function in these patients will allow a normal pregnancy and normal live birth. Recently, Carter *et al.*[24] analyzed pregnancy outcomes of female recipients and female partners of male recipients after hematopoietic stem cell transplantation. Seven females reported 13 pregnancies and 21 males reported 34 pregnancies. Most pregnancies were uncomplicated and resulted in 40 live births. Pregnancy outcomes were compared with those of their nearest-age siblings. The incidence of miscarriage or stillbirth was similar between the two groups. However, a larger study from the European Group for Blood and Marrow Transplantation[25] showed that the incidences of caesarean section, preterm deliverly, and low birthweight singleton birth offspring were higher compared to those in the normal population. Therefore, pregnancies in transplant recipients should be treated as high risks for maternal and fetal complications. In addition, the freezing of ovarian tissues or embryos might have a role as a back-up method of fertility treatment for the patient with ovarian failure after TBI.

We have shown that ovarian function could be preserved by ovarian shielding. However, a longer follow-up is needed to know whether this will allow normal pregnancy and delivery. Also needed is a larger study to evaluate the possible risk of increased relapse of leukemia after transplantation. In addition, the freezing of ovarian tissues or embryos might have a role as a back-up method of fertility preservation for patients who undergo hematopoietic stem cell transplantation and should be evaluated in the future.

References

1 Spinelli S, Chiodi S, Bacigalupo A, Brasca A, Menada MV, Petti AR *et al.* Ovarian recovery after total body irradiation and allogeneic bone marrow transplantation: long-term follow up of 79 females. *Bone Marrow Transplant* 1994; **14**: 373–380.

2 Buskard N, Ballem P, Hill R, Fryer C. Normal fertility after total body irradiation and chemotherapy in conjunction with a bone marrow transplant for acute leukemia. *Clin Invest Med* 1988; **11**: C57.

3 Russell JA, Hanley DA. Full-term pregnancy after allogeneic transplantation for leukemia in a patient with oligomenorrhea. *Bone Marrow Transplant* 1989; **4**: 579–580.

4 Cumber PM, Whittaker JA. Ovarian failure after total body irradiation. *BMJ* 1990; **300**: 464.

5 Calmard-Oriol P, Dauriac C, Vu Van H, Lacroze M, Landriot B, Guyotat D. Successful pregnancy following allogeneic bone marrow transplantation after conditioning by thoraco-abdominal irradiation. *Bone Marrow Transplant* 1991; **8**: 229–230.

6 Giri N, Vowels MR, Barr AL, Mameghan H. Successful pregnancy after total body irradiation and bone marrow

transplantation for acute leukaemia. *Bone Marrow Transplant* 1992; **10**: 93–95.
7 Lipton JH, Derzko C, Fyles G, Meharchand J, Messner HA. Pregnancy after BMT: three case reports. *Bone Marrow Transplant* 1993; **11**: 415–418.
8 Samuelsson A, Fuchs T, Simonsson B, Bjorkholm M. Successful pregnancy in a 28-year-old patient autografted for acute lymphoblastic leukemia following myeloablative treatment including total body irradiation. *Bone Marrow Transplant* 1993; **12**: 659–660.
9 Maruta A, Matsuzaki M, Miyashita H, Kodama F, Kato H, Taguchi J *et al.* Successful pregnancy after allogeneic bone marrow transplantation following conditioning with total body irradiation. *Bone Marrow Transplant* 1995; **15**: 637–638.
10 Wang WS, Tzeng CH, Hsieh RK, Chiou TJ, Liu JH, Yen CC *et al.* Successful pregnancy following very high-dose total body irradiation (1575 cGy) and bone marrow transplantation in a woman with acute myeloid leukemia. *Bone Marrow Transplant* 1998; **21**: 415–417.
11 Chao HT, Wang PH, Yuan CC, Lee WL. Successful pregnancy in a woman with acute myeloid leukemia treated with high-dose whole-body irradiation. *J Reprod Med* 1998; **43**: 703–706.
12 Sanders J. Effects of cyclophosphamide and total body irradiation on ovarian and testicular function (abstract). *Exp Hematol* 1982; **10**: 49.
13 Kanda Y, Oshima K, Asano-Mori Y, Kandabashi K, Nakagawa M, Sakata-Yanagimoto M *et al. In vivo* alemtuzumab enables haploidentical human leukocyte antigen-mismatched hematopoietic stem-cell transplantation without *ex vivo* graft manipulation. *Transplantation* 2005; **79**: 1351–1357.
14 Ban N, Nakaoka H, Haruta R, Murakami Y, Kubo T, Maeda T *et al.* Development of a real-time hand dose monitor for personnel in interventional radiology. *Radiat Prot Dosimetry* 2001; **93**: 325–329.
15 Lawton CA, Barber-Derus SW, Murray KJ, Cohen EP, Ash RC, Moulder JE. Influence of renal shielding on the incidence of late renal dysfunction associated with T-lymphocyte deplete bone marrow transplantation in adult patients. *Int J Radiat Oncol Biol Phys* 1992; **23**: 681–686.
16 Larsen EC, Muller J, Schmiegelow K, Rechnitzer C, Andersen AN. Reduced ovarian function in long-term survivors of radiation- and chemotherapy-treated childhood cancer. *J Clin Endocrinol Metab* 2003; **88**: 5307–5314.
17 Schuck A, Hamelmann V, Bramswig JH, Konemann S, Rube C, Hesselmann S *et al.* Ovarian function following pelvic irradiation in prepubertal and pubertal girls and young adult women. *Strahlenther Onkol* 2005; **181**: 534–539.
18 Shank B, Hoppe RT. Radiotherapeutic principles of hematopoietic cell transplantation. In: Blume KG, Forman SJ, Appelbaum FR (eds). *Thomas's Hematopoietic Cell Transplantation*, 3rd edn. Blackwell Publishing: Malden, MA, USA, 2004, pp 178–197.
19 Sanders JE. Growth and development after hematopoietic stem cell transplantation. In: Blume KG, Forman SJ, Appelbaum FR (eds). *Thomas's Hematopoietic Cell Transplantation*, 3rd edn. Blackwell Publishing: Malden, MA, USA, 2004, pp 929–943.
20 Sanders JE. The impact of marrow transplant preparative regimens on subsequent growth and development. The Seattle Marrow Transplant Team. *Semin Hematol* 1991; **28**: 244–249.
21 Sanders JE, Hawley J, Levy W, Gooley T, Buckner CD, Deeg HJ *et al.* Pregnancies following high-dose cyclophosphamide with or without high-dose busulfan or total-body irradiation and bone marrow transplantation. *Blood* 1996; **87**: 3045–3052.
22 Sanders JE, Buckner CD, Amos D, Levy W, Appelbaum FR, Doney K *et al.* Ovarian function following marrow transplantation for aplastic anemia or leukemia. *J Clin Oncol* 1988; **6**: 813–818.
23 Ringden O, Remberger M, Runde V, Bornhauser M, Blau IW, Basara N *et al.* Peripheral blood stem cell transplantation from unrelated donors: a comparison with marrow transplantation. *Blood* 1999; **94**: 455–464.
24 Carter A, Francisso L, Baker KS, Forman SJ, Grants M, Robinson LL *et al.* Pregnancy outcomes after hematopoietic cell transplantation (HCT). A report from the BMT Survivor Study. *Blood* 2004; **104**, abstr 58.
25 Salooja N, Szydlo RM, Socie G, Rio B, Chatterjee R, Ljungman P *et al.* Late Effects Working Party of the European Group for Blood and Marrow Transplantation. Pregnancy outcomes after peripheral blood or bone marrow transplantation: a retrospective survey. *Lancet* 2001; **358**: 271–276.

GENES, CHROMOSOMES & CANCER 45:482–494 (2006)

Genomewide Screening of DNA Copy Number Changes in Chronic Myelogenous Leukemia with the Use of High-Resolution Array-Based Comparative Genomic Hybridization

Noriko Hosoya,[1,2] Masashi Sanada,[1] Yasuhito Nannya,[1] Kumi Nakazaki,[1] Lili Wang,[1] Akira Hangaishi,[1] Mineo Kurokawa,[1] Shigeru Chiba,[1,2] and Seishi Ogawa[1,3,4]*

[1]Department of Hematology and Oncology, Graduate School of Medicine, University of Tokyo, Tokyo, Japan
[2]Department of Cell Therapy and Transplantation Medicine, University of Tokyo Hospital, University of Tokyo, Tokyo, Japan
[3]Department of Regeneration Medicine for Hematopoiesis, Graduate School of Medicine, University of Tokyo, Tokyo, Japan
[4]Core Research for Evolutional Science and Technology, Japan Science and Technology Corporation, Saitama, Japan

Chronic myelogenous leukemia (CML) evolves from an indolent chronic phase (CP) characterized by the Philadelphia chromosome. Without effective therapy, it progresses to an accelerated phase (AP) and eventually to a fatal blast crisis (BC). To identify the genes involved in stage progression in CML, we performed a genomewide screening of DNA copy number changes in a total of 55 CML patients in different stages with the use of the high-resolution array-based comparative genomic hybridization (array CGH) technique. We constructed Human 1M arrays that contained 3,151 bacterial artificial chromosome (BAC) DNAs, allowing for an average resolution of 1.0 Mb across the entire genome. In addition to common chromosomal abnormalities, array CGH analysis unveiled a number of novel copy number changes. These alterations included losses in 2q26.2–q37.3, 5q23.1–q23.3, 5q31.2–q32, 7p21.3–p11.2, 7q31.1–q31.33, 8pter-p12(p11.2), 9p, and 22q13.1–q13.31 and gains in 3q26.2–q29, 6p22.3, 7p15.2–p14.3, 8p12, 8p21.3, 8p23.2, 8q24.13–q24.21, 9q, 19p13.2–p12, and 22q13.1–q13.32 and occurred at a higher frequency in AP and BC. Minimal copy number changes affecting even a single BAC locus were also identified. Our data suggests that at least a proportion of CML patients carry still-unknown cryptic genomic alterations that could affect a gene or genes of importance in the disease progression of CML. This article contains Supplementary Material available at http://www.interscience.wiley.com/jpages/1045-2257/suppmat.

INTRODUCTION

Chronic myelogenous leukemia (CML) is a clonal disorder originating from pluripotent hematopoietic stem cells that is characterized by the Philadelphia (Ph) chromosome generated by the t(9;22)(q34;q11) (Rowley, 1973; Melo et al., 2003). CML typically shows 3 clinical stages: the initial indolent chronic phase (CP), followed by the intermediate accelerated phase (AP), and then the terminal fatal stage, blast crisis (BC). The prognosis of patients in BC is still very poor, with a median survival of only a few months (Calabretta and Perrotti, 2004). At present, no promising curative therapeutic options are available for patients in BC. The recent development of imatinib mesylate, which selectively inhibits enhanced tyrosine kinase activity of the chimeric BCR–ABL oncoprotein generated by the Ph chromosome, produced impressive therapeutic effects on patients in CP. However, the benefits from this drug seem short-lived once patients progressed to BC (Calabretta and Perrotti, 2004). Thus, to develop new therapeutic approaches for patients in BC, it is essential to identify molecular targets of blastic transformation.

The BC stage of CML is commonly associated with nonrandom secondary chromosomal changes that, in addition to the t(9;22), include +Ph, +8, i(17q), +19, t(3;21)(q26;q22), and t(7;11)(p15;p15) (Prigogina et al., 1978; Alimena et al., 1987; Blick et al., 1987; Melo et al., 2003), or with mutations in

Supported by: Grant-in-Aid for Scientific Research on Priority Areas, Ministry of Education, Culture, Sports, Science and Technology (MEXT); Grant number: KAKENHI 17013022, Grant-in-Aid for Scientific Research, Japan Society for the Promotion of Science (JSPS); Grant number: KAKENHI 16390272, Research on Human Genome, Tissue Engineering, Health and Labour Sciences Research Grants, Ministry of Health, Labour and Welfare; Japan Health Sciences Foundation.

*Correspondence to: Seishi Ogawa, Department of Hematology and Oncology, Department of Regeneration Medicine for Hematopoiesis, Graduate School of Medicine, University of Tokyo, 7-3-1, Hongo, Bunkyo-ku, Tokyo 113-8655, Japan.
E-mail: sogawa-tky@umin.ac.jp

Received 19 October 2005; Accepted 22 November 2005
DOI 10.1002/gcc.20303
Published online 19 January 2006 in Wiley InterScience (www.interscience.wiley.com).

the *TP53*, *CDKN2A*, *RB1*, or *RAS* genes (Ahuja et al., 1989; Kelman et al., 1989; LeMaistre et al., 1989; Feinstein et al., 1991; Nakai et al., 1992, 1994; Mitani et al., 1994; Nakai and Misawa, 1995; Sill et al., 1995; Nakamura et al., 1996; Fioretos et al., 1999; Beck et al., 2000). However, the molecular mechanisms responsible for disease progression in CML have not been fully understood. Array-based comparative genomic hybridization (array CGH) is a robust technology in which a large number of genomic clones are spotted on a glass slide and comparatively hybridized to differentially labeled tumor and reference DNA to enable high-resolution analysis of copy number changes in cancer genomes (Pinkel et al., 1998). Although the array CGH technique has been drawing increasing attention as a tool for studying alterations of genomes in various tumors (Albertson and Pinkel, 2003), it had not been applied to the analysis of patients with CML.

In the present study, to identify genes underlying stage progression in CML, we manufactured Human 1M arrays containing 3,151 bacterial artificial chromosome (BAC) DNAs and performed CGH analysis in 55 primary CML samples in different stages using these arrays. A number of previously unrecognized small cryptic genomic regions were identified.

MATERIALS AND METHODS

PATIENTS AND SAMPLES

After obtaining informed consent, bone marrow or peripheral-blood samples were obtained from 55 Japanese patients diagnosed with CML. Twenty-five of the patients were in the CP stage, 4 were in the AP stage, and 26 were in the BC stage. Clinical details are summarized in Table 1. After approval by the ethical committee at the University of Tokyo, all the samples were subjected to extraction of genomic DNA and anonymized to be used for further analysis according to the regulation of the Japanese government.

Array Fabrication

We constructed Human 1M arrays containing a subset of the FISH (fluorescence in situ hybridization) Mapped Clones V1.3 collection, which were obtained from BACPAC Resources Center (Children's Hospital Oakland Research Institute, Oakland, CA). After excluding clones missing mapping information, a total of 3,151 clones were finally selected for fabrication of Human 1M arrays (Supplementary Table 1; Supplementary material for this article can be found at http://www.interscience.wiley.com/jpages/1045-2257/suppmat), which could be used for genomewide copy number detection at an average resolution of approximately 1.0 Mb. Each BAC DNA was amplified with degenerated oligonucleotide-primed PCR (DOP-PCR) according to the protocol published by Fiegler et al. (2003), with the minor modification of an equimolar combination of DOP 1, 2, and 3 primers being used in the first PCR cycles. Amplified DNA was spotted in duplicate onto GAPS™ II coated slides (Corning, International K.K., Tokyo, Japan), using an Affymetrix 419 Arrayer (Affymetrix, Santa Clara, CA). Before hybridization, array slides were briefly rehydrated over steam and immediately dried on a 75°C heat block. After being baked in a drying oven at 65°C for 3 h and UV-crosslinked at 60 mJ, the slides were rinsed with 0.2× standard saline citrate (SSC) and then with distilled water. The reactive moieties of amino-silane remaining on the glass surface were inactivated for 20 min by gently shaking arrays in a blocking solution, which was freshly prepared by dissolving 4.15 g of succinic anhydride in 245 ml of 1-methyl-2-pyrrolidinone and then adding 22.5 ml of sodium borate (1M, pH 8.0). The slides were briefly rinsed with distilled water and preserved in a desiccator at room temperature, and immediately before hybridization, they were treated in boiling water for 2 min, placed in 100% cold ethanol, and then dried by centrifugation.

DNA Labeling and Hybridization to BAC Arrays

Genomic DNA was extracted from mononuclear cells of the bone marrow or peripheral blood of normal individuals using a PUREGENE™ DNA Isolation Kit (Gentra Systems, Minneapolis, MN). One microgram each of normal reference genomic (male or female) and test DNA were labeled with Cy3-dUTP and Cy5-dUTP, respectively, using a BioPrime® Array CGH Genomic Labeling System (Invitrogen, Carlsbad, CA). After overnight incubation at 37°C, unincorporated nucleotides were removed by use of a BioPrime™ Array CGH Purification Module (Invitrogen, Carlsbad, CA). The labeled test and reference DNA were ethanol-precipitated together with 80 μg of human Cot-1 DNA (Invitrogen, Carlsbad, CA) and 100 μg of yeast tRNA (Roche, Basel, Switzerland), redissolved in a hybridization mix [50% formamide, 5% dextran sulfate, 2× SSC, 5% Tris (pH 7.4), 0.1% Tween 20], and denatured at 75°C for 15 min. After incubation at 37°C for 30 min, the mixture was

TABLE 1. Patient Characteristics, Cytogenetic Description of Their Karyotypes, and Presence of *BCR/ABL* Confirmed by FISH or RT-PCR

Case No.	Sex	Age	Stage	Phenotype	Blast(%)	Karyotype	Methods of *BCR/ABL* detection
AP1	M	51	CML AP		6	46,XY,t(9;22)(q34;q11)(20/20)	NS
AP2	F	56	CML AP		2	50,XX,t(9;22)(q34;q11)+13, +19,+21,+22(8/15) 51,XX,t(9;22)(q34;q11), +t(9;22),+13,+19,+21, +22(4/15) 52,XX,+8,t(9;22)(q34;q11), +t(9;22),+13,+19,+21, +22(2/15) 47,XX,t(9;22)(q34;q11), +19,−20,−21,+der(22) t(9;22),+mar(1/15)	FISH and RT-PCR
AP3	M	37	CML AP		3.3	46,XY,t(9;22)(q34;q11)(18/20) 47,XY,+8,t(9;22)(q34;q11) (2/20)	RT-PCR
AP4	M	74	CML AP		9	46,XY,t(9;22)(q34;q11)(14/20) 45,XY,−21,t(9;22)(q34;q11) (5/20) 45,XY,−17,t(9;22)(q34;q11) (1/20)	RT-PCR
BC1	M	78	CML BC	ND	30	46,XY,t(9;22)(q34;q11)	NS
BC2	M		CML BC	ND	72	46,XY,t(9;22)(q34;q12)	NS
BC3	M	65	CML BC	lymphoid	90	46,XY,t(9;22)(q34;q11)	NS
BC4	M	33	CML BC	lymphoid	70	NA	NS
BC5	M		CML BC	lymphoid	65	NA	NS
BC6	F	48	CML BC	lymphoid	56	46,XX,t(9;22)(q34;q11)	NS
BC7	F	42	CML BC	lymphoid	60	46,XX,t(9;22)(q34;q11)	NS
BC8	F	42	CML BC	lymphoid	70	46,XX,t(9;22)(q34;q11)	NS
BC9	F	60	CML BC	myeloid	98	46,XX,t(9;22)(q34;q11)	NS
BC10	M	62	CML BC	myeloid	90	46,XY,t(9;22)(q34;q11)	NS
BC11	F		CML BC	myeloid	60	NA	NS
BC12	F	53	CML BC	myeloid	20	NA	NS
BC13	F		CML BC	myeloid	88	NA	NS
BC14	M		CML BC	myeloid	75	NA	NS
BC15	M	46	CML BC	myeloid	70	46,XY,t(9;22)(q34;q11)	NS
BC16	M	67	CML BC	myeloid	73	48,XY,t(3;21;18)(q21;q22;p11), +8,t(9;22)(q34;q11), +12(20/20)	FISH and RT-PCR
BC17	F	57	CML BC	myeloid	39	46,XY,t(9;22)(q34;q11)(10/10)	NS
BC18	M	51	CML BC	myeloid	86	46,XY,t(9;22)(q34;q11)(20/20)	FISH and RT-PCR

(Continued)

TABLE 1. Patient Characteristics, Cytogenetic Description of Their Karyotypes, and Presence of *BCR/ABL* Confirmed by FISH or RT-PCR (Continued)

Case No.	Sex	Age	Stage	Phenotype	Blast(%)	Karyotype	Methods of *BCR/ABL* detection
BC19	M	54	CML BC	myeloid	13	NA	FISH and RT-PCR
BC20	M	69	CML BC	myeloid	35	46,XY,t(9;22)(q34;q11)(13/20) 46,XY,t(9;22)(q34;q11),der(12)t(1;12)(q12;q24)(3/20) 46,XY,t(9;22)(q34;q11),der(19)t(1;19)(q12;p13)(4/20)	FISH and RT-PCR
BC21	M	71	CML BC	lymphoid	59	48,XY,11q+,+19,22q−,+22q−(20/20)	RT-PCR
BC22	M	62	CML BC	myeloid	61	46,XY,t(20;22)(p13;q11)(8/20) 47,XY,t(20;22)(p13;q11),+der(22)t(20;22)(p13;q11)(5/20) 45,XY,del(4)(q31),add(6)(p21),der(8;17)(q10;q10),+i(8)(q10),+add(9)(p22),−13,−16,t(20;22)(p13;q11),der(22)t(20;22),inc(1/20) 44,X,−Y,add(6)(p21),der(8;17)(q10;q10),+i(8)(q10),add(9)(p22),−13,−16,t(20;22)(p13;q11),inc(1/20) 74–87, ND, including add(6)(p21),der(8;17)(q10;q10),add(9)(p22),t(20;22)(p13;q11)(5/20)	RT-PCR
BC23	M	28	CML BC	myeloid	36	46,XY,t(9;22)(q34;q11)(18/20) 46,XY(2/20)	FISH and RT-PCR
BC24	M	60	CML BC	myeloid	44	48,XY,+8,t(9;22)(q34;q11),+der(22)t(9;22)(q34;q11)(19/20) 50,XY,+8,+8,t(9;22)(q34;q11),+21,+der(22)t(9;22)(q34;q11)(1/20)	FISH and RT-PCR
BC25	M	37	CML BC	myeloid	28	46,XY,t(9;22)(q34;q11)(12/20) 46,XY(8/20)	FISH and RT-PCR
BC26	M	64	CML BC	myeloid	85	45,XY,add(5)(q15),der(9)t(9;22)(q34;q11),add(12)(p11),del(17)(p11),add(19)(q13),−21,der(22)add(22)(p11)t(9;22)(17/20)	FISH and RT-PCR

(Continued)

TABLE 1. Patient Characteristics, Cytogenetic Description of Their Karyotypes, and Presence of *BCR/ABL* Confirmed by FISH or RT-PCR (Continued)

Case No.	Sex	Age	Stage	Phenotype	Blast(%)	Karyotype	Methods of *BCR/ABL* detection
						45,XY,der(5)t(5;21)(q31;q11), der(9)t(9;22)(q34;q11), del(17)(p11),add(19)(q13), −21,der(22)add(22)(p11) t(9;22)(1/20) 48,XY,dup(3)(q21q27),add(4) (q21),der(5)t(5;21)(q31;q11), t(9;22)(q34;q11),add(13)(p11), del(17)(p11),+19,−21, +der(22)t(9;22),+mar(1/20) 48,XY,dup(3)(q21q27),−4, der(5)t(5;21)(q31;q11), t(9;22)(q34;q11),add(13)(p11), del(17)(p11),+19,−21, +der(22)t(9;22),+mar(1/20)	
CP1	M	40	CML CP		0	46,XY,t(9;22)(q34;q11)	NS
CP2	M	28	CML CP		0	NA	NS
CP3	F	60	CML CP		0	46,XX,t(9;22)(q34;q11)	NS
CP4	M	62	CML CP		0	46,XY,t(9;22)(q34;q11)	NS
CP5	M	38	CML CP		5	46,XY,t(9;22)(q34;q11)	NS
CP6	M	35	CML CP		5	46,XY,t(9;22)(q34;q11)	NS
CP7	M	54	CML CP		0	46,XY,t(9;22)(q34;q11)	NS
CP8	F		CML CP		0	NA	NS
CP9	M		CML CP		0	46,XY,t(9;22)(q34;q11)	NS
CP10	M		CML CP		1	46,XY,t(9;22)(q34;q11)	NS
CP11	F	32	CML CP		0	46,XX,t(9;22)(q34;q11)	NS
CP12	F	59	CML CP		0	46,XX,t(9;22)(q34;q11)	NS
CP13	M	51	CML CP		0	46,XY,t(9;22)(q34;q11)	NS
CP14	F		CML CP		0	46,XX,t(9;22)(q34;q11)	NS
CP15	M	46	CML CP		0	46,XY,t(9;22)(q34;q11)	NS
CP16	M	58	CML CP		0	46,XY,t(9;22)(q34;q11)	NS
CP17	F	58	CML CP		0	46,XX,t(9;22)(q34;q11)	NS
CP18	F	74	CML CP		0	46,XX,t(9;22)(q34;q11)	NS
CP19	F	54	CML CP		0	46,XX,t(9;22)(q34;q11)	NS
CP20	M		CML CP		0.5	46,XY,t(9;22)(q34;q11)	NS
CP21	M	71	CML CP		0	46,XY,t(9;22)(q34;q11)(20/20)	NS
CP22	M	40	CML CP		0	46,XY,t(9;22)(q34;q11)(20/20)	FISH and RT-PCR
CP23	M	43	CML CP		1.5	46,XY(20/20)	FISH and RT-PCR
CP24	F	55	CML CP		2	46,XX,t(9;22)(q34;q11)(20/20)	NS
CP25	M	75	CML CP		0	46,XY,t(9;22)(q34;q11)	NS

ND: not determined; NA: information not available; NE: not examined; NS: not specified in clinical records; Ph chr: Philadelphia chromosome; chr: chromosome; RT-PCR: reverse-transcriptase-polymerase-chain-reaction; The t(20;22)(p13;q11) in case BC26 is a variant Ph translocation.

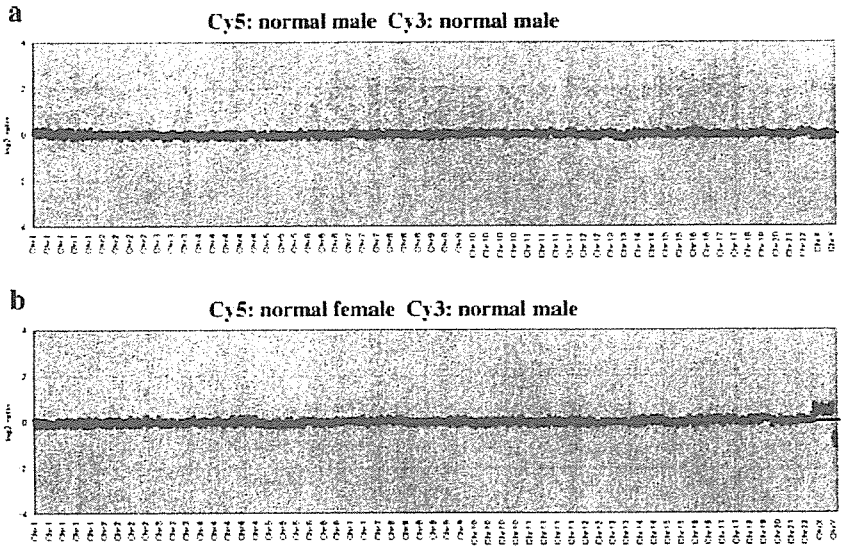

Figure 1. Representative array CGH results obtained from reference-versus-reference control hybridization. Clones are ordered from chromosomes 1 to 22, X, and Y and within each chromosome according to the UCSC mapping position (http://genome.ucsc.edu/; May 2004 draft). Each spot represents an average $\log_2$ signal ratio for each BAC locus. (a) For all loci, $\log_2$ ratios were within the thresholds −0.2 and 0.2 in the male-versus-male control experiment. (b) Gain in chromosome X (0.435 ± 0.124) and loss in chromosome Y (−0.807 ± 0.167) were clearly visualized in the female-versus-male control experiment (Cy5 and Cy3, respectively).

applied to an array slide placed in a MAUI® Mixer AO Hybridization Chamber Lid (BioMicro Systems, Salt Lake City, UT) and incubated at 37°C for 60–66 h using a MAUI Hybridization System (BioMicro Systems). After hybridization, the slides were washed once in a solution of 50% formamide and 2× SSC for 15 min at 50°C and once in 2× SSC for 15 min at room temperature. Slides were rinsed briefly with 0.2× SSC and dried immediately by centrifugation.

Image Analysis and Processing

After hybridization, the arrays were scanned by an Affymetrix 428™ Array Scanner (Affymetrix, Santa Clara, CA). The scanned image was analyzed by an ImaGene v4.2 (BioDiscovery, Inc., Marina Del Rey, CA) in order to extract Cy3 and Cy5 signals for each spot, and after local background signals were subtracted, test/reference $\log_2$ ratios of the test and reference signals were calculated for all spots. The $\log_2$ ratios were normalized so that the average $\log_2$ ratio of all spots became zero. A spot was eliminated from the analysis if the signal intensity after the background subtraction in either Cy5 or Cy3 was less than −18 decibels or the duplicated signals differed by more than 0.4 in the $\log_2$ ratios. The average $\log_2$ ratios of the two replicate spots were calculated for the remaining spots. An experiment was not adopted if less than 90% of all spots met the above-mentioned criteria or if the standard deviation (SD) of all spots was larger than 0.25. Thresholds for copy number gain and loss were defined as $\log_2$ ratios of +2 SD and −2 SD, respectively. The reproducibility of the data was confirmed in two independent experiments for each tumor sample. For two representative cases, the consistency of the CGH results was confirmed by dye-swap experiments, in which tumor and reference DNA were inversely labeled with Cy3 and Cy5, respectively.

FISH Analysis

Interphase FISH experiments were performed as previously described (Wang et al., 2003).

RESULTS

Quality Test of BAC Array

Prior to the analysis of CML samples, control experiments were performed to evaluate the quality of the Human 1M array, in which DNA from normal individuals was used as a test sample. In the male-versus-male control hybridizations, $\log_2$ ratios for all spots were within the thresholds of −0.2 and 0.2 (Fig. 1a), whereas in the female-versus-male hybridizations, copy number gain of the whole chromosome X and copy number loss of the whole chromosome Y were detected successfully (Fig. 1b). In the latter experiments, the mean $\log_2$ ratios of the clones on the X and Y chromosomes were 0.435 ± 0.124 and −0.807 ± 0.167, respectively, compared to the mean $\log_2$ ratio of −0.008 ± 0.083 for all clones from autosomal chromosomes.

Higher Frequency of DNA Copy Number Changes in CML in BC and AP

A total of 55 CML samples in different stages were analyzed for copy number alterations by array CGH using Human 1M arrays. Table 2 lists the copy number alterations detected in individual

TABLE 2. Gains and Losses Detected by Array CGH

Case No.	Regions and clones that showed copy number gains	Regions and clones that showed copy number losses
AP1	3q26.2–q29 (RP11-91A17~RP11-233N20), 7p15.2–p14.3 (RP11-81F15~RP11-89N17)	22q13.2–q13.31 (RP11-81N15~RP11-66M5)
AP2	9p21.2 (RP11-81B19)-qter, Chromosome13, Chromosome19, Chromosome21, Chromosome22, ***22q11.1–q11.22 and 9q34.13–qter*** 22q13.1–q13.32 (RP11-4H24-RP11-133P21)	**8p23.1 (RP11-287P18)**
AP3	**5p15.1 (RP11-88L18, RP11-90B23), 19p13.2 (RP11-79F15)**	none
AP4	**8q21.2 (RP11-90G23)**	none
BC1	none	none
BC2	none	none
BC3	**4p15.33 (RP11-143120), 5p15.1 (RP11-88L18)** 8p12 (RP11-274F14-RP11-100B16), 9q, **19p13.2 (RP11-79F15)**, ***22q11.1–q11.22 and 9q34.13–qter***	**1q25.1 (RP11-177M16)**, 5q23.1–q23.3 (RP11-47L19-RP11-89G4), 5q31.2–q32 (RP11-11514~RP11-88H2), 7q31.1–q31.33 (RP11-79G19~RP11-90C13), 8pter–p12 (RP11-91P13), 9p
BC4	**8p23.1 (RP11-287P18), 22q11.21 (RP11-278E23)**	none
BC5	**8p23.1 (RP11-287P18), 17p13.3 (RP11-582C6), 19p13.2 (RP11-79F15)**	**17q21.31 (RP11-52N13)**
BC6	none	**5p15.1 (RP11-88L18)**
BC7	Chromosome8	none
BC8	none	none
BC9	none	**21q22.12 (RP11-17O20)**
BC10	**8p23.1 (RP11-287P18), 17p13.3 (RP11-582C6)**	none
BC11	none	none
BC12	**8p23.1 (RP11-287P18), 17p13.3 (RP11-582C6)**	**5p15.1 (RP11-88L18)**
BC13	none	Chromosomes 4 and 13
BC14	Chromosome8, **8q21.2 (RP11-90G23)**	none
BC15	**8p23.1 (RP11-287P18)**	none
BC16	Chromosome8*, **8p23.1 (RP11-287P18)**, Chromosome12*, **17p13.3 (RP11-582C6)**, ***22q11.1–q11.2 and 9q34.13–qter***	2q36.2–q37.3 (RP11-68H19~RP11-90E11*), 18pter–q11.2 (RP11-79F3)*
BC17	none	**1q25.3 (RP11-196B7), 17q21.31 (RP11-52N13)**
BC18	none	**1q25.3 (RP11-173E24), 1q25.3–q31.1 (RP11-162L13)**
BC19	none	**5p15.1 (RP11-88L18)**, 7p21.3–p11.2 (RP11-79O21~RP11-90N11)
BC20	none	**9q22.32 (RP11-223A21)**
BC21	**5p15.1 (RP11-88L18)**, Chromosome19*, ***22q11.1–q11.2 and 9q34.13–qter***	none
BC22	6p22.3 (RP11-43B4~RP11-288M24), 8p21.3 (RP11-89O4~RP11-274M9), 8p11.21 (RP11-282J24)-qter	8pter–p11.2 (RP11-284J3)
BC23	**5p15.1 (RP11-88L18)**	none
BC24	Chromosome8*, **17p13.3 (RP11-582C6), 17q22 (RP11-143M4)** ***22q11.1–q11.2 and 9q34.13–qter***	**5p15.1 (RP11-88L18), 7q11.21 (RP11-90C3)**
BC25	**5p15.1 (RP11-88L18), 19p13.2 (RP11-79F15)**	none
BC26	8q24.13–q24.21 (RP11-229L23-RP11-237F24), 19p13.2–p12 (RP11-84C17~RP11-91L5), ***22q11.1–q11.2 and 9q34.13–qter***	none
CP1	**8p23.1 (RP11-287P18), 17p13.3 (RP11-582C6)**	**1q25.1 (RP11-177M16), 1q25.3 (RP11-173E24), 5p15.1 (RP11-88L18)**
CP2	**17q21.31 (RP11-52N13)**	**1q25.1 (RP11-177M16)**
CP3	**17p13.3 (RP11-582C6), 17q12(CTD-2019C10)**	**5p15.1 (RP11-88L18), 17q25.2 (RP11-145C11)**

(Continued)

TABLE 2. Gains and Losses Detected by Array CGH (Continued)

Case No.	Regions and clones that showed copy number gains	Regions and clones that showed copy number losses
CP4	**5p15.1 (RP11-88L18), 19p13.2 (RP11-79F15)**	**1q25.1 (RP11-177M16), 17q21.31 (RP11-52N13)**
CP5	none	none
CP6	none	**5p15.1 (RP11-88L18)**
CP7	**19p13.2 (RP11-79F15)**	none
CP8	none	Chromosome3
CP9	none	none
CP10	none	none
CP11	none	none
CP12	**6q25.3–q26 (RP11-43B19)**	none
CP13	**8p23.1 (RP11-287P18), 17p13.3 (RP11-582C6)**	none
CP14	**19p13.2 (RP11-79F15)**	none
CP15	8p23.2 (RP11-113B7~RP11-89I12), **8p23.1 (RP11-287P18), *22q11.1–q11.2 and 9q34.13–qter***	none
CP16	**19p13.2 (RP11-79F15)**	**8q21.2 (RP11-90G23)**
CP17	none	none
CP18	**17p13.3 (RP11-582C6)**, 17p11.2–qter	**17q12(CTD-2019C10)** 17pter–p12
CP19	none	none
CP20	**19p13.2 (RP11-79F15)**	**5p15.1 (RP11-88L18)**
CP21	**8p23.1 (RP11-287P18), 15q22.31 (RP11-50N10), 22q13.32 (RP11-133P21)**	**1q25.1 (RP11-177M16)**
CP22	none	none
CP23	none	none
CP24	none	**5p15.1 (RP11-88L18, RP11-90B23), 8q21.3 (RP11-91K2), 9q32 (RP11-95J4)**
CP25	none	none

22q11.1–11.2 and ***9q34.13–qter*** corresponds to Philadelphia chromosome.
Gain of 17p11.2–qter together with loss of 17pter–p12 represents isochromosome 17q (i(17q)).
Copy number changes involving a single BAC are indicated in bold. Underlined are the regions (or BAC loci) whose copy number changes were confirmed by FISH.

cases, and Table 3 summarizes the number of cases showing each copy number alteration in different stages of CML. Array CGH successfully detected cryptic gains and losses that had been missed by conventional karyotyping analysis as well as large chromosomal changes that had been observed in prior conventional karyotyping analysis (Tables 2 and 3).

When analysis was confined to copy number alterations that involved at least two consecutive BAC clones, only 4 copy number alterations were detected in 25 patients in CP, whereas 38 copy number alterations were identified in 30 patients in AP/BC (Table 2). The frequency of DNA copy number alterations was significantly higher in AP/BC than in CP ($P < 0.005$).

Large and Small Cryptic Changes Detected by High-Resolution Array CGH

In the current analysis, the most frequent alteration was gain of extra Ph chromosomes (6 cases in AP/BC, 1 case in CP), which was inferred from gains of a distal part of 9q and a proximal part of 22q. Alterations of whole chromosomes, including gains of chromosomes 8 (4 cases in BC), 19 (2 cases in AP/BC), 13, 21, and 22 (1 case each in AP), and losses of chromosomes 3 (1 case in CP), 4, and 13 (1 case each in BC) were also observed (Tables 2 and 3). One CP patient (case CP18) displayed both gain of 17p11.2–qter and loss of 17pter–p12 material, suggesting the presence of an isochromosome 17q—i(17q)—which has repeatedly been reported in association with CML BC (Prigogina et al., 1978; Alimena et al., 1987; Fioretos et al., 1999; Melo et al., 2003), although the conventional karyotyping analysis had missed this abnormality.

Our array CGH analysis also uncovered cryptic changes that had not been reported in CML and therefore were novel regions implicated in the pathogenesis and progression of CML. Case BC3 was found to have a balanced t(9;22) translocation as the sole chromosomal abnormality in karyotyp-

TABLE 3. Summary of Copy Number Alterations Detected by Array CGH

	Stage	
	CP ($n = 25$)	AP + BC ($n = 30$)
Gains		
Unbalanced translocations or gains that were also detected by G-banding analysis		
Ph (22q11.1–q11.2 and 9q34.13–qter)	0	3
Chromosome 8	0	2
Chromosome 13	0	1
Chromosome 19	0	2
Chromosome 21	0	1
Chromosome 22	0	1
Gains in cases in which G-banding analysis was not done		
Chromosome 8	0	1
3q26.2–q29	0	1
7p15.2–p14.3	0	1
8p11.21–q24.3	0	1
Cryptic gains that were not detected by G-banding analysis (involving at least two consecutive BAC clones spotted on the array)		
Ph (22q11.1–q11.2 and 9q34.13–qter)	1	3
i(17q) (gain of 17p11.2–qter and loss of 17pter–p12)	1	0
Chromosome 8	0	1
6p22.3	0	1
8p12	0	1
8p21.3	0	1
8p23.2	1	0
8q24.13–q24.21	0	1
9p21.2–qter	0	1
9q	0	1
19p13.2–p12	0	1
22q13.1–q13.32	0	z1
Total number	3	26
Losses		
Losses in cases in which G-banding analysis was not done		
Chromosome 3	1	0
Chromosome 4	0	1
Chromosome 13	0	1
7p21.3–p11.2	0	1
22q13.1–q13.31	0	1
Cryptic losses that were not detected by G-banding analysis (involving at least two consecutive BAC clones spotted on the array)		
2q36.2–q37.3	0	1
5q23.1–q23.3	0	1
5q31.2–q32	0	1
7q31.1–q31.33	0	1
8pter–p12	0	1
8pter–p11.2	0	1
9p	0	1
18pter–q11.2	0	1
Total number	1	12

ing analysis (Tables 1 and 2). However, in array CGH, multiple copy number alterations, including gains in 8p12 and 9q, and an extra Ph chromosome, and losses in 5q23.1–q23.3, 5q31.2–q32, 7q31.1–q31.33, 8pter–p12, and 9p were reproducibly detected in duplicate experiments (Table 2, Fig. 2a). Case BC16 had a karyotype showing 48,XY, t(3;21;18)(q21;q22;p11),+8, t(9;22)(q34;q11), +12 (Table 1), whereas array CGH also detected an extra Ph chromosome as well as losses in 2q36.2–q37.3 and 18pter–q11.2 (Table 2, Fig. 2b). Also, in case BC22, CGH analysis disclosed cryptic copy number gains in three consecutive BACs within a small 6p22.3 region spanning 505 kb (Table 2, Fig. 2c).

These array CGH results were confirmed by FISH analysis using affected BAC clones as probes when Carnoy samples were available (Table 2, Fig. 2b and c). For example, the sample from patient BC16 showed, consistent with trisomies 8 and 12, three signals from clones RP11-150N13, on chromosome 8 (with an average $\log_2$ ratio of 0.449), and RP11-91I15, on chromosome 12 (with an average $\log_2$ ratio of 0.474), whereas clones RP11-116M19, on chromosome 2 (with an average $\log_2$ ratio of −0.538), and RP11-105C15, on chromosome 18 (with an average $\log_2$ ratio of −0.701), produced only one signal, confirming the presence of an allelic deletion in these regions (Fig. 2b). In patient BC22, clones RP11-228M24, at 6p22.3 (with an average $\log_2$ ratio of 1.158), showed multiple signals, in agreement with the copy number gain found in array CGH (Fig. 2c).

Copy number changes that involved only a single BAC locus (Table 4) were verified by FISH analysis for selected cases (Table 2 and Fig. 2d). In total, 75 single BAC copy number changes (SBCs) were identified in 24 BAC loci among 55 CML patients. Because 35 of the 75 SBCs, found in three BAC loci, were also identified in normal individuals (3 SBCs, at RP11-88L18, RP11-287P18, and RP11-586C6, in 10 healthy Japanese individuals; data not shown) and 37 SBCs in six BAC loci appeared as both copy number gains and losses depending on samples, suggesting that many of these are likely to represent polymorphisms known as large-scale copy number variations (LCVs; Iafrate et al., 2004; Sebat et al., 2004; Table 4). Indeed, 11 of the 24 BAC loci showing SBCs conformed to regions previously reported as LCVs (Table 4) (Iafrate et al., 2004; Sebat et al., 2004).

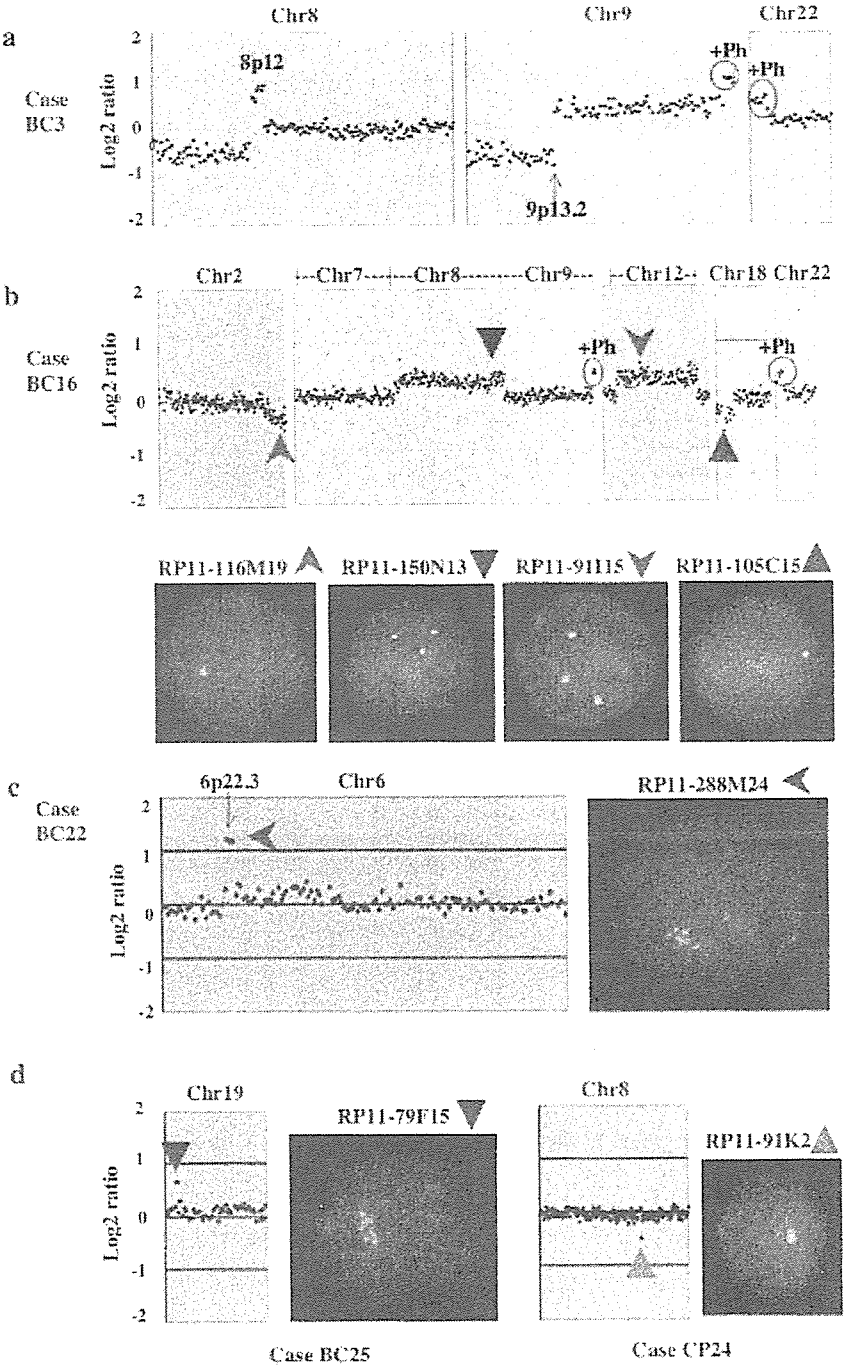

Figure 2. Gains and losses detected by array CGH and confirmed by FISH analysis. (a) Array CGH profile of case BC3, showing an extra Ph chromosome, gains in 8p12 and 9q and losses in 8pter–8p12 and 9p, not detected by karyotyping analysis; (b) Array CGH profile of case BC16, in which an extra Ph chromosome, gain in chromosome 8 with a higher-level of gain of the clone RP11-287P18, gain in chromosome 12, and losses in 2q36.2–2q37.3 and 18pter–18q11.2 were identified. Interphase FISH analysis of this case used the indicated biotin-labeled BAC clones as probes. Consistent with trisomies 8 and 12, clones RP11-150N13, on chromosome 8 (average $\log_2$ ratio of 0.449), and RP11-91I15, on chromosome 12 (average $\log_2$ ratio of 0.474), showed 3 signals, whereas clones RP11-116M19, on chromosome 2 (average $\log_2$ ratio of −0.538), and RP11-105C15, on chromosome 18 (average $\log_2$ ratio of −0.701), produced only one signal, confirming an allelic deletion in these regions. (c) Array CGH profile of case BC22, for which clone RP11-288M24, at chromosome 6p22.3 (average $\log_2$ ratio of 1.158), showed multiple signals, confirming copy number gains in this region. (d) Array CGH profiles of cases BC25 and CP24, in which single BAC copy number changes were observed. Copy number gain (RP11-79F15) and loss (RP11-91K2) were verified by FISH analysis.

Candidate Genes Implicated in Pathogenesis or Disease Progression of CML

The regions showing gain or loss in DNA copy number or breakpoint regions of unbalanced chromosomal translocations could harbor one or more genes implicated in the pathogenesis of CML or disease progression to BC. Supplementary Table 2 lists the representative genes within these regions identified in this study, not including the single BAC regions showing both gains and losses. Among previously reported cellular oncogenes or leukemia-related genes were *EVI1* (3q26), *FGFR1* (8p12), and *MYC* (8q24), which were included in the regions showing copy number gains in 3q26.2–q29, 8p12, and 8q24.13–q24.21, respectively (Supplementary Table 2). The 505-kb region showing

TABLE 4. Copy Number Alterations Involving a Single BAC Locus

	Stage	
	CP ($n = 25$)	AP + BC ($n = 30$)
Gains		
4p15.33 (RP11-143I20)[a]	0	1
5p15.1 (RP11-88L18)[a]	1	5
5p15.1 (RP11-90B23)	0	1
6q25.3–q26 (RP11-43B19)[a]	1	0
8p23.1 (RP11-287P18)[a]	4	6
8q21.2 (RP11-90G23)[a]	0	2
15q22.31 (RP11-50N10)	1	0
17p13.3 (RP11-582C6)[a]	4	5
17q12 (CTD-2019C10)	1	0
17q21.31 (RP11-52N13)	1	0
17q22 (RP11-143M4)	0	1
19p13.2 (RP11-79F15)[a]	4	4
22q11.21 (RP11-278E23)[a]	0	1
22q13.32 (RP11-133P21)	1	0
Losses		
1q25.1 (RP11-177M16)	4	1
1q25.3 (RP11-196B7)	0	1
1q25.3 (RP11-173E24)	1	1
1q25.3–q31.1 (RP11-162L13)	0	1
5p15.1 (RP11-88L18)[a]	5	4
5p15.1 (RP11-90B23)	1	0
7q11.21 (RP11-90C3)[a]	0	1
8p23.1 (RP11-287P18)[a]	0	1
8q21.2 (RP11-90G23)[a]	1	0
8q21.3 (RP11-91K2)[a]	1	0
9q32 (RP11-95J4)[a]	1	0
9q22.32 (RP11-223A21)	0	1
17q12 (CTD-2019C10)	1	0
17q21.31 (RP11-52N13)	1	2
17q25.2 (RP11-145C11)	1	0
21q22.12 (RP11-17O20)	0	1

Shaded areas point to the loci that showed both gains and losses in different samples.
[a]Regions previously reported to show large-scale copy number variations (LCVs).

copy number gain at the chromosome band 6p22.3 contained *OACT1* (*O*-acetyltransferase domain containing 1) and *E2F3* (E2F transcription factor 3), both known genes (Supplementary Table 2). It is not clear whether this region overlapped with the breakpoint region of the recurrent translocations t(6;19)(p22;q13) and t(6;9;22)(p22;q34;q11) in CML (Huret et al., 1989; Meza Espinoza et al., 2004; Yehuda et al., 1999), because the precise molecular breakpoints at 6p22 in these cases have not been characterized. The 346-kb region at 8p23.2 that showed copy number gain includes *CSMD1* (CUB and sushi multiple domains protein 1 precursor), the only transcriptome (Supplementary Table 2). Other abnormalities newly identified in this study involved mostly large regions of 2q26.2–q37.3 (16.8 Mb), 5q23.1–q23.3 (10.6 Mb), 5q31.2–q32 (6.50 Mb), 7p15.2–p14.3 (6.14 Mb), 7p21.3–p11.2 (41.7 Mb), 7q31.1-q31.33 (17.9 Mb), 8p21.3 (2.18 Mb), and 19p13.2–p12 (12.1 Mb), which made it difficult to pinpoint the candidate target genes.

DISCUSSION

In this article, we have shown genomewide detection of DNA copy number changes in a total of 55 CML patients at different stages using high-resolution array CGH. Using this technique, we delineated not only previously reported abnormalities, but also novel alterations involving narrow regions that may harbor only one or several candidate genes involved in the pathogenesis or disease progression of CML.

A number of cryptic copy number alterations that had been missed by karyotyping analysis were detected in array CGH analysis. Seven patients were found to have extra Ph chromosomes, which was the most frequent alteration in our series, although this alteration had not been detected by prior G-banding analysis in four of the seven patients (57%). In addition, more than 10 novel, cryptic copy number alterations were uncovered at a significantly higher frequency in patients in BC and AP, suggesting that these regions may contain genes relevant to the pathogenesis of CML, especially in progressive stages. Considering the wide variety of copy number alterations detected in AP/BC cases and that the majority of these abnormalities were observed in a single patient in our series, there might be a large heterogeneity in the molecular pathogenesis of CML AP/BC cases, and it may be possible that analysis of a larger number of patients could disclose novel recurrent molecular defects in CML. Alternatively, the genes included in the affected regions may also be deregulated by other mechanisms such as point mutations or epigenetic effects, which could not be detected by copy number analysis.

Many of the cryptic gains or losses affecting a single BAC locus are thought to represent copy number polymorphisms or LCVs rather than tumor-specific changes, and given their high frequency, it would be difficult to discriminate tumor-specific changes from LCVs. In our analysis, SBCs (or LCVs) seemed to be more frequently found in CML than in normal individuals using the same reference set (55 of 75 in CML vs. 3 of 10 in normal individuals, $P = 0.021$). Although

recent reports suggested a possible association of some LCVs with the regions implicated in cancer development (Iafrate et al., 2004; Sebat et al., 2004), the precise role of the LCVs detected in the current analysis in the pathogenesis of CML is still unclear and should be addressed in future studies that would include a larger number of normal subjects.

Although array CGH analysis successfully unveiled cryptic genomic aberrations in CML, we should note that it also has limitations in that the tumor content of the samples clearly affected the sensitivity of detecting copy number changes in tumor components. According to our admixture experiments, in which mixed tumor and normal DNA were tested for detection of a trisomy, the threshold of tumor content for detection of trisomies in our array CGH was estimated to be more than 20%–40% tumor components (data not shown). Thus, the trisomy 8 in AP3 and the monosomy 21 in AP4 as revealed by G-banding analysis were not expected to be detected in array CGH analysis because abnormal metaphases were found in only 2 of 20 with AP3 and 5 of 20 with AP4 (Tables 1 and 2). On the other hand, array CGH failed to detect the loss of chromosome 21 found in 17 of 20 metaphases in G-banding analysis in BC26, which was most likely a result of karyotypic overrepresentation of one or more rapidly proliferating tumor subclones in G-banding analysis. Finally, the FISH Mapped Clones V1.3 collection distributed from BACPAC Resources Center, which we used for array construction, does not cover some regions of particular interest in CML pathogenesis. For example, deletions of the 5′ region of the *ABL/BCR* junction on the der(9) chromosome, which is known to affect 10%–15% of the CML patients (Storlazzi et al., 2002), were missed in this study because our Human 1M arrays did not contain BAC clones including the *ABL* gene or the upstream *ASS* gene.

In conclusion, our array CGH analysis disclosed not only common chromosomal abnormalities, but also small, cryptic copy number alterations in CML genomes that were not detected by conventional analysis. It enabled a better description of genetic alterations in CML, which potentially could be applicable to molecular diagnostics and prediction of disease prognosis of this neoplastic disorder. The submicroscopic copy number alterations detected in this study might contribute to the identification of novel molecular targets implicated in the pathogenesis or disease progression of CML. Further studies with whole-genome tiling arrays having much higher resolutions will help to detect precisely the genes involved in the disease progression of CML.

ACKNOWLEDGMENTS

We are grateful to the late professor Hisamaru Hirai (Department of Hematology and Oncology, University of Tokyo) for his encouragement in this work. We dedicate this paper to his memory. We also thank Ms. Yasuko Ogino and Mr. Kenjirou Masuda (Lab Company Limited, Tokyo, Japan) for their technical assistance.

REFERENCES

Ahuja H, Bar-Eli M, Advani SH, Benchimol S, Cline MJ. 1989. Alterations in the p53 gene and the clonal evolution of the blast crisis of chronic myelocytic leukemia. Proc Natl Acad Sci USA 86:6783–6787.

Albertson DG, Pinkel D. 2003. Genomic microarrays in human genetic disease and cancer. Hum Mol Genet 12 Spec No 2:R145–R152.

Alimena G, De Cuia MR, Diverio D, Gastaldi R, Nanni M. 1987. The karyotype of blastic crisis. Cancer Genet Cytogenet 26:39–50.

Beck Z, Kiss A, Toth FD, Szabo J, Baesi A, Balogh E, Borbely A, Telek B, Kovacs E, Olah E, Rak K. 2000. Alterations of P53 and RB genes and the evolution of the accelerated phase of chronic myeloid leukemia. Leuk Lymphoma 38:587–597.

Blick M, Romero P, Talpaz M, Kurzrock R, Shtalrid M, Andersson B, Trujillo J, Beran M, Gutterman J. 1987. Molecular characteristics of chronic myelogenous leukemia in blast crisis. Cancer Genet Cytogenet 27:349–356.

Calabretta B, Perrotti D. 2004. The biology of CML blast crisis. Blood 103:4010–4022.

Feinstein E, Cimino G, Gale RP, Alimena G, Berrhier R, Kishi K, Goldman J, Zaccaria A, Berrebi A, Canaani E. 1991. p53 in chronic myelogenous leukemia in acute phase. Proc Natl Acad Sci USA 88:6293–6297.

Fiegler H, Carr P, Douglas EJ, Burford DC, Hunt S, Scott CE, Smith J, Vetrie D, Gorman P, Tomlinson IP, Carter NP. 2003. DNA microarrays for comparative genomic hybridization based on DOP-PCR amplification of BAC and PAC clones. Genes Chromosomes Cancer 36:361–374.

Fioretos T, Strombeck B, Sandberg T, Johansson B, Billstrom R, Borg A, Nilsson PG, Van Den Berghe H, Hagemeijer A, Mitelman F, Hoglund M. 1999. Isochromosome 17q in blast crisis of chronic myeloid leukemia and in other hematologic malignancies is the result of clustered breakpoints in 17p11 and is not associated with coding TP53 mutations. Blood 94:225–232.

Huret JL, Schoenwald M, Brizard A, Guilhot F, Vilmer E, Tanzer J. 1989. Chromosome 6p rearrangements appear to be secondary changes in various haematological malignancies. Leuk Res 13:819–824.

Iafrate AJ, Feuk L, Rivera MN, Listewnik ML, Donahoe PK, Qi Y, Scherer SW, Lee C. 2004. Detection of large-scale variation in the human genome. Nat Genet 36:949–951.

Kelman Z, Prokocimer M, Peller S, Kahn Y, Rechavi G, Manor Y, Cohen A, Rotter V. 1989. Rearrangements in the p53 gene in Philadelphia chromosome positive chronic myelogenous leukemia. Blood 74:2318–2324.

LeMaistre A, Lee MS, Talpaz M, Kantarjian HM, Freireich EJ, Deisseroth AB, Trujillo JM, Stass SA. 1989. Ras oncogene mutations are rare late stage events in chronic myelogenous leukemia. Blood 73:889–891.

Melo JV, Hughes TP, Apperley JF. 2003. Chronic myeloid leukemia. Hematology (Am Soc Hematol Ed Prog):132–152.

Meza Espinoza JP, Judith Picos Cardenas V, Gutierrez-Angulo M, Gonzalez Garcia JR. 2004. Secondary chromosomal changes in 34 Philadelphia-chromosome-positive chronic myelocytic leukemia patients from the Mexican West. Cancer Genet Cytogenet 148:166–169.

Mitani K, Ogawa S, Tanaka T, Miyoshi H, Kurokawa M, Mano H, Yazaki Y, Ohki M, Hirai H. 1994. Generation of the AML1-EVI-1 fusion gene in the t(3;21)(q26;q22) causes blastic crisis in chronic myelocytic leukemia. Embo J 13:504–510.

Nakai H, Misawa S. 1995. Chromosome 17 abnormalities and inactivation of the p53 gene in chronic myeloid leukemia and their prognostic significance. Leuk Lymphoma 19:213–221.

Nakai H, Misawa S, Taniwaki M, Horiike S, Takashima T, Seriu T, Nakagawa H, Fujii H, Shimazaki C, Maruo N and others. 1994. Prognostic significance of loss of a chromosome 17p and p53 gene mutations in blast crisis of chronic myelogenous leukaemia. Br J Haematol 87:425–427.

Nakai H, Misawa S, Toguchida J, Yandell DW, Ishizaki K. 1992. Frequent p53 gene mutations in blast crisis of chronic myelogenous leukemia, especially in myeloid crisis harboring loss of a chromosome 17p. Cancer Res 52:6588–6593.

Nakamura T, Largaespada DA, Lee MP, Johnson LA, Ohyashiki K, Toyama K, Chen SJ, Willman CL, Chen IM, Feinberg AP, Copeland NG, Jenkins NA, Shaughnessy JD Jr. 1996. Fusion of the nucleoporin gene NUP98 to HOXA9 by the chromosome translocation t(7;11)(p15;p15) in human myeloid leukaemia. Nat Genet 12:154–158.

Pinkel D, Segraves R, Sudar D, Clark S, Poole I, Kowbel D, Collins C, Kuo WL, Chen C, Zhai Y, Dairkee SH, Ljung BM, Gray JW, Albertson DG. 1998. High resolution analysis of DNA copy number variation using comparative genomic hybridization to microarrays. Nat Genet 20:207–211.

Prigogina EL, Fleischman EW, Volkova MA, Frenkel MA. 1978. Chromosome abnormalities and clinical and morphologic manifestations of chronic myeloid leukemia. Hum Genet 41:143–156.

Rowley JD. 1973. Letter: A new consistent chromosomal abnormality in chronic myelogenous leukaemia identified by quinacrine fluorescence and Giemsa staining. Nature 243:290–293.

Sebat J, Lakshmi B, Troge J, Alexander J, Young J, Lundin P, Maner S, Massa H, Walker M, Chi M, Navin N, Lucito R, Healy J, Hicks J, Ye K, Reiner A, Gilliam TC, Trask B, Patterson N, Zetterberg A, Wigler M. Large-scale copy number polymorphism in the human genome. Science 305:525–528.

Sill H, Goldman JM, Cross NC. 1995. Homozygous deletions of the p16 tumor-suppressor gene are associated with lymphoid transformation of chronic myeloid leukemia. Blood 85:2013–2016.

Wang L, Ogawa S, Hangaishi A, Qiao Y, Hosoya N, Nanya Y, Ohyashiki K, Mizoguchi H, Hirai H. 2003. Molecular characterization of the recurrent unbalanced translocation der(1;7)(q10;p10). Blood 102:2597–2604.

Yehuda O, Abeliovich D, Ben-Neriah S, Sverdlin I, Cohen R, Varadi G, Orr R, Ashkenazi YJ, Heyd J, Lugassy G, Ben Yehuda D. 1999. Clinical implications of fluorescence in situ hybridization analysis in 13 chronic myeloid leukemia cases: Ph-negative and variant Ph-positive. Cancer Genet Cytogenet 114:100–107.

Journal of Antimicrobial Chemotherapy (2006) **57**, 1004–1007
doi:10.1093/jac/dkl089
Advance Access publication 21 March 2006

JAC

Pharmacokinetics of ganciclovir in haematopoietic stem cell transplantation recipients with or without renal impairment

Yuki Asano-Mori[1], Yoshinobu Kanda[1,2]*, Kumi Oshima[1,2], Takuro Watanabe[1], Eriko Shoda[1], Toru Motokura[1], Mineo Kurokawa[1,2] and Shigeru Chiba[1,2]

[1]*Department of Hematology & Oncology, University of Tokyo Graduate School of Medicine and Hospital, Tokyo, Japan;*[2]*Department of Cell Therapy & Transplantation Medicine, University of Tokyo Hospital, Tokyo, Japan*

Received 3 October 2005; returned 22 November 2005; revised 25 January 2006; accepted 24 February 2006

***Objectives*: We investigated the pharmacokinetics of ganciclovir in 12 haematopoietic stem cell transplantation (HSCT) recipients to evaluate the validity of a 50% reduction in the ganciclovir dosage for mild renal impairment.**

***Patients and methods*: Ganciclovir at 5 mg/kg/day was pre-emptively infused in patients with estimated $CL_{CR} \geq 70$ mL/min (Group A), whereas the dose was reduced to 2.5 mg/kg/day in patients with CL_{CR} between 50 and 70 mL/min (Group B).**

***Results*: The peak concentration was significantly higher in Group A ($P < 0.01$). However, the decrease in the plasma ganciclovir concentration was slower in Group B ($P = 0.09$), and the AUC of all patients in both groups was distributed within a narrow range (25.6 ± 4.77 μg·h/mL), when two patients with exceptionally high AUC values were excluded.**

***Conclusions*: A 50% reduction in ganciclovir appeared to be appropriate for patients with mild renal impairment. Measuring the ganciclovir concentration at 4 h after starting infusion may be adequate for evaluating AUC.**

Keywords: cytomegalovirus, CMV, antigenaemia, antiviral therapy

Introduction

Ganciclovir is the mainstay of antiviral agents in pre-emptive therapy against cytomegalovirus (CMV) disease after allogeneic haematopoietic stem cell transplantation (HSCT).[1] Ganciclovir is mainly excreted from the kidney and about 90% of the administered dose is recovered unchanged in the urine after intravenous (iv) administration.[2] Therefore, total body clearance correlates well with CL_{CR}.[3,4] In HSCT settings, patients frequently develop renal impairment caused by the use of nephrotoxic drugs. A 50% reduction of ganciclovir is recommended in the drug information leaflet for patients with mild renal impairment of CL_{CR} between 50 and 70 mL/min in order to achieve an unchanged AUC. However, the pharmacokinetic profiles of ganciclovir have not yet been fully evaluated in such patients. Therefore, we investigated the validity of this dose reduction by serial evaluation of the plasma ganciclovir concentration.

Patients and methods

Twelve patients (nine men and three women) aged between 23 and 61 years were enrolled in a 12 h pharmacokinetic study of intravenous ganciclovir after ethical approval. The median age and weight were 50.5 years (range 23–61) and 57.5 kg (range 36.7–80.0), respectively. All patients provided informed consent to participate in this study. The underlying disease was acute leukaemia in three patients, chronic myelogenous leukaemia in three patients, myelodysplastic syndrome in two patients and pancreatic cancer in four patients. Five patients received a graft from an HLA-matched relative and seven received a graft from an alternative donor defined as an HLA-mismatched relative or a matched unrelated donor. We calculated CL_{CR} weekly, based on a 24 h urine collection. Patients were classified into two groups according to CL_{CR} evaluated within 1 week before the initiation of ganciclovir administration: Group A included seven patients with $CL_{CR} \geq 70$ mL/min (mean 98.1 mL/min, range 74.9–142.0 mL/min) and Group B included five patients

*Corresponding author. Tel: +81-3-3815-5411 ext. 35602; Fax: +81-3-5804-6261; E-mail: ycanda-tky@umin.ac.jp

JAC antiviral

Table 1. Pharmacokinetic parameters of ganciclovir in Groups A and B

	Group A (CL_{CR} ≥ 70 mL/min)	Group B (CL_{CR} 50–70 mL/min)	*P* value
C0.5	6.56 (4.39–11.33) μg/mL	4.92 (2.90–10.80) μg/mL	0.37
C1	9.20 (5.50–19.03) μg/mL	4.75 (3.32–6.61) μg/mL	<0.01
C2	4.76 (2.72–12.09) μg/mL	2.38 (2.30–2.73) μg/mL	<0.01
C4	2.58 (1.25–6.30) μg/mL	1.57 (1.37–1.80) μg/mL	0.17
C6	1.69 (0.79–4.89) μg/mL	1.15 (0.90–1.30) μg/mL	0.29
C8	1.22 (0.40–3.99) μg/mL	0.91 (0.64–1.09) μg/mL	0.57
C12	0.62 (0.23–2.88) μg/mL	0.58 (0.39–0.81) μg/mL	0.94
LogC4/C1	–0.66 (–0.73– –0.48)	–0.42 (–0.68– –0.33)	0.09
AUC	29.8 (20.2–111.0) μg·h/mL	24.6 (22.5–28.3) μg·h/mL	0.57
$t_{1/2}$	3.57 (3.36–7.94) h	5.76 (5.05–8.87) h	0.03
CL_{TOT}	3.04 (0.73–4.31) mL/min/kg	1.66 (1.50–1.81) mL/min/kg	0.12

CL_{CR}, creatinine clearance; AUC, area under the concentration curve; $t_{1/2}$, elimination half-life; CL_{TOT}, total body clearance.
C0.5–C12 represent plasma ganciclovir concentrations at 30 min, and 1, 2, 4, 6, 8 and 12 h after start of infusion, respectively.
The values of each parameter are reported as the median and range.

with CL_{CR} between 50 and 70 mL/min (mean 59.1 mL/min, range 51.3–67.4 mL/min).

Antigenaemia assay for CMV infection was performed weekly after engraftment as described previously.[5] Ganciclovir was pre-emptively started when 20 or more positive cells were detected per two slides in patients who received a graft from an HLA-matched relative, whereas it was started when three or more positive cells were detected per two slides in patients who received a graft from an alternative donor. The starting dose of ganciclovir was once daily at 5 and 2.5 mg/kg/day in Groups A and B, respectively, which was infused at a constant rate over 1 h.[6] Venous blood samples were obtained before infusion (C0), 30 min (C0.5) and 1 (C1), 2 (C2), 4 (C4), 6 (C6), 8 (C8) and 12 (C12) h after starting the first-dose infusion. After the blood sample was centrifuged, the plasma was separated and stored at –20°C until measurement of the ganciclovir concentration.

The plasma ganciclovir concentration was measured after solid-phase extraction (SPE) and dilution in mobile phase by reversed-phase HPLC. In brief, plasma samples were heated at 58°C for 30 min to inactivate the virus prior to handling. These samples were then diluted with 0.1 M phosphate buffer (pH 8.0) and applied to disposable C_{18} SPE columns (Bond Elut C18-OH; Varian, Palo Alto, CA, USA) conditioned with methanol and water. The column was washed with 0.1 M phosphate buffer (pH 8.0) and water, and ganciclovir was then eluted by 1.5 mL of 15% methanol. After 0.1 mL of 10 μg/mL guanosine was added as an internal standard, the eluent was injected into the HPLC system (C_{18} column, CAPELL PAK C18 SG 120; Shiseido, Tokyo, Japan; mobile phase: a mixture of 20 mM KH_2PO_4 (pH 2.6) containing 5 mM sodium 1-octanesulfonate and acetonitrile (95 : 5, v/v)]. The flow rate of the mobile phase and the column temperature were 0.8 mL/min and 40°C, respectively. The HPLC was equipped with a photo diode array detector (SPD-M10A vp, Shimadzu, Kyoto, Japan) set at a detection wavelength of 254 nm. This quantitative assay provided a high selectivity for determining a compound in biological samples. It was available for 0.02–5 μg/mL of an analyte in plasma samples. The precision expressed as a coefficient of variation was less than 2.5%, and the accuracy expressed as an error per cent was <±3%. Endogenous sources of interference were not detected from blank plasma.

Pharmacokinetic parameters were calculated by non-compartment modelling using WinNonlin software (version 4.0; Pharsight Corporation). CL_{CR} was normalized to 1.73 m^2 body surface area and AUC was calculated using the linear trapezoidal rules with extrapolation to infinity by standard techniques. The decline ratio was calculated as Log C4/C1 for the evaluation of the decrease in plasma ganciclovir concentration in the distribution phase and early elimination phase, whereas the elimination half-life was calculated from the terminal portion of the slope after C4. The differences between groups were compared using the Wilcoxon (Mann–Whitney)-test. *P* values of less than 0.05 were considered statistically significant. The relationship between the total AUC and plasma ganciclovir concentration at each point after starting infusion was investigated by calculating correlation coefficients r^2 using linear regression analysis after logarithmic transformation because they did not fit a normal distribution.

Results

The median pharmacokinetic parameters and the concentration versus time profile are shown in Table 1 and Figure 1(a). The peak plasma concentration (C_{max}) ranged from 3.32 to 19.03 μg/mL. The C_{max} in Group A was significantly higher than that in Group B (9.20 versus 4.75 μg/mL, $P < 0.01$). There was a borderline significance in the decline ratio between the two groups (–0.66 versus –0.42, $P = 0.09$). Total body clearance in Group B was lower than that in Group A (1.66 versus 3.04 mL/min/kg, $P = 0.12$). Also, the elimination half-life in Group B was significantly longer than that in Group A (5.76 versus 3.57 h, $P = 0.03$). There was no significant difference in AUC between the two groups (29.8 versus 24.6 μg·h/mL, $P = 0.57$). The AUCs of the patients in both groups were distributed within a narrow range (25.6 ± 4.77 μg·h/mL, Figure 1b), when we excluded two patients with exceptionally high AUC values (48.18 and 110.99 μg·h/mL). The CL_{CR} values of these two patients were 74.9 and 87.2 mL/min, respectively. Among the serial ganciclovir concentration measurements, C4 most strongly correlated with AUC ($r^2 = 0.95$, Figure 1c).

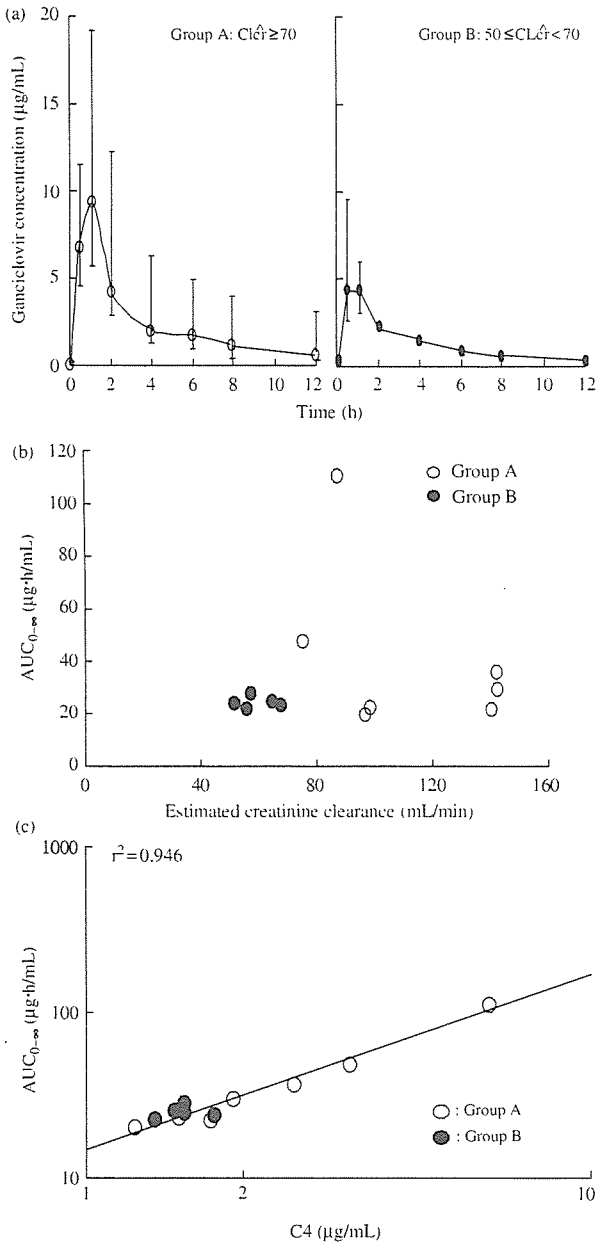

Figure 1. (a) Median concentrations of ganciclovir after 1 h iv infusion of 5 mg/kg ganciclovir in Group A and of 2.5 mg/kg ganciclovir in Group B. Open and filled circles represent each median concentration point in Groups A and B, respectively. (b) The AUC in each patient. Open and filled circles represent individual measurements in Groups A and B, respectively. (c) Correlation between the AUC and the plasma concentration at 4 h after starting infusion (C4). Open and filled circles represent individual measurements in Groups A and B, respectively. The solid line represents the orthogonal regression line described by the equation AUC = 17.666 × C4 − 4.4555.

Discussion

The results demonstrated that a 50% reduction in the ganciclovir dosage was appropriate for HSCT recipients with mild renal impairment of CL_{CR} between 50 and 70 mL/min. In addition to the significant difference in the elimination half-life, we observed a difference in the decline ratio (Log C4/C1) between the two groups with a borderline significance, which might indicate that renal excretion had started within 4 h of infusion. AUC was not significantly different from that in patients with normal renal function, probably due to the prolonged elimination in patients with mild renal impairment, although the small sample size might be responsible for the lack of significant difference. When we excluded two patients whose AUC values were exceptionally high, the AUC ranged within 25.6 ± 4.77 μg·h/mL, which was similar to the values reported previously.[4] An exceptionally high AUC was observed in two patients with CL_{CR} values between 70 and 90 mL/min. The reason for the high AUC is not clear, but it may suggest that the dose of ganciclovir should be reduced in patients with CL_{CR} values between 70 and 90 mL/min after confirming that the AUC is significantly high in such patients. Drug interaction is also a possible explanation for the high AUC, but these two patients were not being given drugs that are known to interact with ganciclovir. Also, the exceptionally high AUC might result from a transient renal dysfunction, which could not be detected even by a weekly CL_{CR} examination.

The role of clinical pharmacokinetic monitoring in solid organ transplantation as well as in HSCT is unclear.[7] Previous studies failed to show a significant correlation between the ganciclovir concentration and its efficacy or toxicity.[7,8] A possible explanation for this lack of correlation is the small number of patients in these studies, since a significant correlation between the cumulative dose of ganciclovir and the incidence of neutropenia has been shown in large-scale clinical studies.[9,10] However, it is difficult to perform a large-scale study with pharmacokinetic monitoring because of the need for repeated blood sampling from patients. In this study, C4 most strongly correlated with AUC, with r^2 values of 0.95, although we should confirm this in a larger study. Another limitation of pharmacokinetic monitoring of ganciclovir is that only the intracellular phosphorylated ganciclovir is active and it is not known how its concentration relates to the plasma concentrations. Nevertheless, a prospective study with monitoring of C4 is warranted to evaluate the role of pharmacokinetic monitoring in HSCT.

In conclusion, a recommended reduction of ganciclovir dosage by 50% appeared to be appropriate for HSCT recipients with mild renal impairment. Measurement of the plasma ganciclovir concentration C4 could be an accurate predictor of AUC. Further studies are necessary to validate these findings in a larger number of patients and to clarify the relationship among plasma concentrations, AUC and responses.

Transparency declarations

None to declare.

References

1. Forman SJ, Zaia JA. Treatment and prevention of cytomegalovirus pneumonia after bone marrow transplantation: where do we stand? *Blood* 1994; **83**: 2392–8.

2. Shepp DH, Dandliker PS, de Miranda P *et al.* Activity of 9-[2-hydroxy-1-(hydroxymethyl)ethoxymethyl]guanine in the treatment of cytomegalovirus pneumonia. *Ann Intern Med* 1985; **103**: 368–73.

3. Fletcher C, Sawchuk R, Chinnock B *et al.* Human pharmacokinetics of the antiviral drug DHPG. *Clin Pharmacol Ther* 1986; **40**: 281–6.

4. Sommadossi JP, Bevan R, Ling T *et al.* Clinical pharmacokinetics of ganciclovir in patients with normal and impaired renal function. *Rev Infect Dis* 1988; S507–14.

5. Gondo H, Minematsu T, Harada M *et al.* Cytomegalovirus (CMV) antigenaemia for rapid diagnosis and monitoring of CMV-associated disease after bone marrow transplantation. *Br J Haematol* 1994; **86**: 130–7.

6. Kanda Y, Mineishi S, Saito T *et al.* Response-oriented preemptive therapy against cytomegalovirus disease with low-dose ganciclovir: a prospective evaluation. *Transplantation* 2002; **73**: 568–72.

7. Scott JC, Partovi N, Ensom MHH. Ganciclovir in solid organ transplant recipients: is there a role for clinical pharmacokinetic monitoring? *Ther Drug Monit* 2004; **26**: 68–77.

8. Erice A, Jordan MC, Chace BA *et al.* Ganciclovir treatment of cytomegalovirus disease in transplant recipients and other immunocompromised host. *JAMA* 1987; **257**: 3082–7.

9. Buhles WJ, Mastre BJ, Tinker AJ *et al.* Ganciclovir treatment of life- or sight-threatening cytomegalovirus infection: experience in 314 immunocompromised patients. *Rev Infect Dis* 1988; S495–506.

10. Kanda Y, Mineishi S, Saito T *et al.* Pre-emptive therapy against cytomegalovirus (CMV) diseases guided by CMV antigenemia assay after allogeneic hematopoietic stem cell transplantation: a single-center experience in Japan. *Bone Marrow Transplant* 2001; **27**: 437–44.

Ann Hematol (2006) 85: 523–529
DOI 10.1007/s00277-006-0114-4

ORIGINAL ARTICLE

Hideomi Yamashita · Koji Izutsu · Naoki Nakamura · Kenshiro Shiraishi · Shigeru Chiba · Mineo Kurokawa · Masao Tago · Hiroshi Igaki · Kuni Ohtomo · Keiichi Nakagawa

Treatment results of chemoradiation therapy for localized aggressive lymphomas: a retrospective 20-year study

Received: 29 January 2006 / Accepted: 24 February 2006 / Published online: 12 May 2006

Abstract In this study we analyzed our cases of localized aggressive lymphoma treated in our institution during the last 20 years to compare the finding of this study with those of previous studies. Forty patients with Ann Arbor stage I–II aggressive lymphoma were treated with 3–6 cycles of a CHOP regimen (cyclophosphamide, doxorubicin, vincristine, and prednisolone) and radiation therapy (30 or 40 Gy with involved field). Between 1985 and 2003, 40 patients with stage I (N=25) or stage II (N=15) disease were treated. Chemotherapy mainly preceded radiotherapy, although the sequence of radiotherapy and chemotherapy was determined by individual physicians and patients' choice. Median and mean age was 50.5 and 48.6 years, respectively, at the time of diagnosis, with a male to female ratio of 19:21. Analyses were undertaken to determine (1) response to treatment according to age, international prognostic index (IPI), lactate dehydrogenase (LDH) value, serum interleukin 2 receptor (sIL-2R) value, cell type, stage, extent of maximum local disease, with or without mediastinal lymph nodes, number of sites, anatomic distribution, and irradiation dose, and (2) relapse patterns. Complete follow-up was obtained in all patients. The follow-up period of surviving 33 patients ranged from 24.7 to 180 months with a median of 69 and a mean of 72.7 months. A complete remission (CR) was achieved in 37 patients (93%). A study of relapse patterns after a CR showed that four patients had a first relapse within a radiation field and the other one patient had an extranodal distant relapse. Significant prognostic factors were not identified by multivariate analysis. Combined chemotherapy and radiation therapy is safe, highly effective, and probably curative for most patients with stage I–II aggressive lymphoma.

Keywords Aggressive lymphoma · Stage I–II · Combined chemotherapy and radiation therapy · CHOP regimen · Localized lymphoma · Non-Hodgkin's lymphoma

H. Yamashita · N. Nakamura · K. Shiraishi · M. Tago · H. Igaki · K. Ohtomo · K. Nakagawa (✉)
Department of Radiology,
University of Tokyo Hospital,
7-3-1 Hongo,
Bunkyo-ku, Tokyo 113-8655, Japan
e-mail: nakagawa-rad@umin.ac.jp
Tel.: +81-3-58008667
Fax: +81-3-58008935

K. Izutsu · S. Chiba · M. Kurokawa
Department of Hematology–Oncology,
University of Tokyo Hospital,
Tokyo, Japan

Introduction

Throughout the past 25 years, the treatment of limited-stage diffuse aggressive non-Hodgkin's lymphoma has evolved from surgical staging and radiotherapy (RT) to primary chemotherapy (CTx) and limited RT [1–5].

Some investigators have suggested that adjunctive RT is not indicated for most patients in the management of DLCL [6–8]. Others, in an effort to reduce the incidence of local recurrence and possibly improve survival, have added RT to their CTx programs particularly for patients with bulky or other unfavorable Stage II presentations [9–16].

CHOP (cyclophosphamide, doxorubicin, vincristine and prednisone) has been used as a standard CTx for DLBCL and 3 cycles of CHOP followed by RT has also been accepted for localized DLBCL [17]. There are many reports that favor adjuvant chemotherapy with involved-field RT even for with localized lymphoma [18–21]. This article describes the usefulness of RT combined with CTx in the management of localized aggressive lymphoma.

Materials and methods

Patients

This is a retrospective study. The subjects were 40 patients with localized aggressive lymphoma and treated with combined CTx using CHOP regimen and RT for curative intent as the primary therapy. The cases in which the World